IOP Conf. Series: Materials Science and Engineering **200** (2017) 012038 doi:10.1088/1757-899X/200/1/012038

Modelling pressure rolling of asymmetric rolling process

V Alexa, S A Ratiu, I Kiss and V G Cioata

University Politehnica Timisoara, Faculty of Engineering Hunedoara, Department of Engineering and Management, Hunedoara, Romania

E–mail: vasile.alexa@fih.upt.ro

Abstract. The paper presents a comparative analysis between experimental results and modelling in order to interpret the value of the contact pressure on the asymmetric longitudinal rolling. It is also intended action and the different behaviour of upper cylinder compared to the lower cylinder action in situations when both are driven, or only one operates. In the modelling will be presented on the basis of boundary conditions imposed rolling pressure variation in the degree of reduction and also re size arc length of contact. Determining a curve is also important to determine the locus of points which characterize symmetry conditions partial rolling process between unequal diameters cylinders.

1. Establishing engineering mathematical models for the rolling process

This paper is part of the modern trends of gradual replacement of the physical experiments with numerical ones in the design and optimisation of the technological processes of plastic deformation by rolling. By its nature, this paper requires a multidisciplinary approach, starting with the deep understanding of the theory of complex phenomena of metallic materials plastic deformation by rolling, and continuing with the modern techniques of processing and interpretation of the experimentally obtained data.

1.1. The model used for the contact arc length [1]

The length of the contact arc between the metallic material and the rolls is one of the decisive parameters influencing the strength, temperature and kinematic conditions of the rolling process. To determine the length of the contact arc for symmetrical and asymmetrical cold rolling, in addition to the roll reduction and radius, we must also know the elastic deformations of the rolls and the strip undergoing the rolling process, values that depend on the strength of the rolling process.

This problem can be solved by using the rolling theory equations, as well as the elasticity theory equations, based on the well-known models and methods for calculating the length of the contact arc for cold rolling.

Using the Hertz's concept (relationship 1), a number of models have been obtained, as following:

$$l_c = \sqrt{\frac{2 \cdot R_1 \cdot R_2}{R_1 + R_2} \Delta h} \tag{1}$$

a) The *Hitchcock's* model, which takes into account the elastic compression of the rolls:

$$l_c = x_{lc} + \sqrt{R \cdot \Delta h + x_{lc}^2} \tag{2}$$

$$x_{lc} = 8 \cdot p_{mc} \cdot R \cdot \theta_c \tag{3}$$

$$\theta_c = \frac{1-\gamma_c^2}{\pi \cdot E_c} \quad (4)$$

R – the radius of the working rolls*;*
Δh – the absolute reduction;
p_{mc} – the mean normal contact stress;
γ_c – the Poisson's ratio;
E_c – the elastic modulus of the material which the rolls are made of
Relationship 2 does not take into account the elastic deformations of the strip undergoing the rolling process, and the normal stress diagram is adopted in the shape of semi ellipse.
b) *The Roberts* model takes into account the contact between the rolls and an ideal rigid plan:

$$l_c = \sqrt{R \cdot \Delta h} + 1{,}08\sqrt{\frac{2 \cdot R \cdot p_b}{E_c}} \quad (5)$$

p_b – The normal force acting per unit length of the strip;
c)*Ţelicov and Grişcov* proposed the following relationship to calculate the increase of the contact arc length by taking into account the asymmetry of the normal stresses diagram:

$$x_{lc} = 8 \cdot p_{mc} \cdot R \cdot \theta_c \quad (6)$$

This relationship (6) helps reducing the errors between the calculated values and the experimental ones.
d) The *Ţelicov's* model introduces also the influence of elastic deformations of the strip:

$$l_c = x_l + \sqrt{R \cdot \Delta h + x_l^2} \quad (7)$$

$$x_{lc} = 8 \cdot p_{mc} \cdot R \cdot (\theta_c + \theta_b) \quad (8)$$

$$\theta_b = \frac{1-\gamma_b^2}{\pi \cdot E_b} \quad (9)$$

The mean normal contact stress, the contact arc length and its increase along the plane passing through the centres of the rolls are calculated by taking into account the elastic deformations of the rolls and the strip;
e) *Dinnik* shows in his model that the determination of the contact arc length increase x_l without taking into account the length of the strip and the diagram symmetry for normal stresses is irrational, proposing x_l to be determined using the relationship:

$$x_l = 0{,}5 \cdot a \cdot x_{lc}\left(1 + \sqrt{1 + 1{,}74\frac{h_l}{x_{lc}}}\right) \quad (10)$$

a – Coefficient considering the asymmetry of the normal stresses diagrams:
h_l – Thickness of the strip after rolling
For determining the value of x_{lc}, Dinnik recommends the Relationship 3.
f) The relationship proposed by *Cepurchin* determines the contact arc length taking into account only the elastic compression of the rolls, as follows:

$$l_c = \sqrt{R \cdot \Delta h + c \cdot p_b \cdot \theta_c \cdot R} \quad (11)$$

c – Shape coefficient of the normal stresses diagram
g) Based on the previous model, *Poluhin* obtained the dependence for determining the length of the contact arc by taking into account the elastic deformations of the rollers and strip. Therefore:

$$l_c = \sqrt{R \cdot \Delta h + c_1 \cdot p_b \cdot (\theta_c + \theta_b) \cdot R} \quad (12)$$

Where:

$$c_1 = 8 + 2\sqrt{\frac{4 \cdot \Delta h}{p_b(\theta_c + \theta_b)} + 16} \quad (13)$$

1.2. The model used for the mean normal contact stresses [1]

Since the elastic deformations of the strips are neglected in all the proposed models, we are going to analyse the plastic contact portion between the strip and the rolls to determine the mean contact pressure.

Thus, there are a number of models proposed in the literature, which are distinguished by simplicity and compactness, and are obtained considering a constant value of the resistance to deformation for the mean values of the respective parameters. The models proposed by these authors, without taking into account the influence of elastic deformations of the rolls, are shown in the following table:

Table 1. The variation domains of variables

Stone	$p_m = \beta \cdot \sigma_{cm} \cdot \frac{E^{f\frac{1}{h_m}} - 1}{f\frac{1}{h_m}}$	(14)
Bland and Ford	$p_m = \beta \cdot \sigma_{cm}\left(1{,}08 + 1{,}79 \cdot \varepsilon \cdot f \cdot \sqrt{\frac{R}{\Delta h}} - 1{,}02 \cdot \varepsilon\right)$	(15)
Roberts	$p_m = \beta \cdot \sigma_{cm}\left(1 - 1{,}25 \cdot \varepsilon + \frac{f \cdot l}{2 \cdot h_m}\right)\frac{1}{1-\varepsilon}$	(16)
Lugovschi	$p_m = \beta \cdot \sigma_{cm}\left(1 + \frac{f \cdot l}{2 \cdot h_m}\right)$	(17)
Telikov	$p_m = \frac{\beta \cdot \sigma_{cm}}{\Delta h}\left\{\frac{h_0}{\delta - 2}\left[\left(\frac{h_0}{h_n}\right)^{\delta-2} - 1\right] + \frac{h_1}{\delta + 2}\left[\left(\frac{h_n}{h_{n1}}\right)^{\delta+2} - 1\right]\right\}$	(18)

where:

$$\delta = \frac{2 \cdot f \cdot l}{\Delta h} \quad (19)$$

$$l = \sqrt{R \cdot \Delta h} \quad (20)$$

$$h_n = \sqrt[2\delta]{h_0^{\delta-1} \cdot h_1^{\delta+1}} \quad (21)$$

$$\Delta h = h_0 - h_1 \quad (22)$$

$$\varepsilon = \frac{\Delta h}{h_0} \quad (23)$$

For the convenience of further analysis of the model, we replace the "p_m" value with the dimensionless parameter "*n*", which is the stress state coefficient:

$$n_\sigma = \frac{p_m}{\beta \cdot \sigma_c} \quad (24)$$

And dependencies: for determining: $l, \delta, \frac{h_1}{\Delta h}, h_n, \frac{h_0}{h_n}, \frac{h_n}{h_1}$ and h_m:

$$l = \sqrt{R\Delta h} = h_0\sqrt{\frac{R}{h_0} \cdot \varepsilon} \quad (25)$$

$$\delta = \frac{2 \cdot f \cdot l}{\Delta h} = 2 \cdot f \cdot \sqrt{\frac{R}{h_0} \cdot \frac{1}{\varepsilon}} \quad (26)$$

$$\frac{h_1}{\Delta h} = \frac{1-\varepsilon}{\varepsilon} \quad (27)$$

$$h_n = \sqrt[2\delta]{h_0^{\delta-1} \cdot h_1^{\delta+1}} = h_0\sqrt[2\delta]{(1-\varepsilon)^{\delta+1}} \quad (28)$$

$$\frac{h_0}{h_1} = \frac{h_0}{h_0 \sqrt[2\delta]{(1-\varepsilon)^{\delta+1}}} = \frac{1}{\sqrt[2\delta]{(1-\varepsilon)^{\delta+1}}} \tag{29}$$

$$\frac{h_n}{h_1} = \frac{h_0 \sqrt[2\delta]{(1-\varepsilon)^{\delta+1}}}{h_0 - \Delta h} = \frac{1}{1-\varepsilon} \sqrt[2\delta]{(1-\varepsilon)^{\delta+1}} \tag{30}$$

$$h_m = 0{,}5(h_0 + h_1) = 0{,}5(2-\varepsilon)h_0 \tag{31}$$

With consideration of relations, models of the Table 1, take the form

Table 2. The variation domains of variables

Stone	$n_\sigma = \frac{1}{\frac{2 \cdot f \cdot \sqrt{\frac{R}{h_0}} \cdot \varepsilon}{2-\varepsilon}} \left(E^{\frac{2 \cdot f \cdot \sqrt{\frac{R}{h_0}} \cdot \varepsilon}{2-\varepsilon}} - 1 \right)$	(32)
Bland and Ford	$n_\sigma = 1{,}08 + 1{,}79 \cdot \varepsilon \cdot f \cdot \sqrt{\frac{R}{h_0} \cdot \frac{1}{1-\varepsilon}} - 1{,}02 \cdot \varepsilon$	(33)
Roberts	$n_\sigma = \left(1 - 1{,}25 \cdot \varepsilon + \frac{f}{2} \sqrt{\frac{R}{h_0} \cdot \varepsilon} \right) \frac{1}{1-\varepsilon}$	(34)
Lugovschi	$n_\sigma = \left(1 + \frac{f}{2-\varepsilon} \sqrt{\frac{R}{h_0} \cdot \varepsilon} \right)$	(35)
Telikov	$n_\sigma = \frac{1}{\varepsilon(\delta-2)} \left\{ \left[\frac{1}{\sqrt[2\delta]{(1-\varepsilon)^{\delta+1}}} \right]^{\delta-2} - 1 \right\} + \frac{1-\varepsilon}{\varepsilon(\delta+2)} \left\{ \left[\frac{1}{1-\varepsilon} \sqrt[2\delta]{(1-\varepsilon)^{\delta+1}} \right]^{\delta+2} - 1 \right\}$	(36)

Dependencies can be simplified to some extent, if adopted:

$$A = f \sqrt{\frac{R}{h_0}} \tag{37}$$

$$\delta = 2A \sqrt{\frac{1}{\varepsilon}} \tag{38}$$

After entering in we obtain:

Table 3. The variation domains of variables

Stone	$n_\sigma = \frac{1}{\frac{2A\sqrt{\varepsilon}}{2-\varepsilon}} \left(E^{\frac{2A\sqrt{\varepsilon}}{2-\varepsilon}} - 1 \right)$	(39)
Bland and Ford	$n_\sigma = 1{,}08 + 1{,}79 \cdot \varepsilon \cdot A \cdot \sqrt{\frac{1}{1-\varepsilon}} - 1{,}02 \cdot \varepsilon$	(40)
Roberts	$n_\sigma = \left(1 - 1{,}25 \cdot \varepsilon + \frac{A}{2} \sqrt{\varepsilon} \right) \frac{1}{1-\varepsilon}$	(41)
Lugovschi	$n_\sigma = \left(1 + \frac{A}{2-\varepsilon} \sqrt{\varepsilon} \right)$	(42)
Telikov	$n_\sigma = \frac{1}{\varepsilon(\delta-2)} \left\{ \left[\frac{1}{\sqrt[2\delta]{(1-\varepsilon)^{\delta+1}}} \right]^{\delta-2} - 1 \right\} + \frac{1-\varepsilon}{\varepsilon(\delta+2)} \left\{ \left[\frac{1}{1-\varepsilon} \sqrt[2\delta]{(1-\varepsilon)^{\delta+1}} \right]^{\delta+2} - 1 \right\}$	(43)

The relationships confirm the fact that the stress state coefficient "*n*", found in all the analysed models, finally represents a function of three dimensionless parameters:

1 – the coefficient of friction;

2 – the ratio between the radius of the working rolls and the thickness of the bar at the entrance into the deformation zone;

3 – the relative reduction, which is also the criterion of similarity;

2. The experimental plant and testing method

The research for this theme purpose have been made on a 170 mm reversing two-high rolling mill, created and installed in the no conventional technologies and plastic deformation laboratory of the Engineering Faculty from Hunedoara [1-3].

Figure 1, [1] shows a general view of the installation, which has been built by the author of this paper and which, compared to all the other mills, allows a simultaneous registering of the symmetric and asymmetric rolling process parameters, which are the rolling force (F_d and F_a), the side efforts (X_d and X_a), the pressure on the surface of contact with the superior roll (p_{ms}) and the with inferior one (p_{mi}), the real lengths of the springs of contact with the superior roll (l_s) and with the inferior one (l_i).

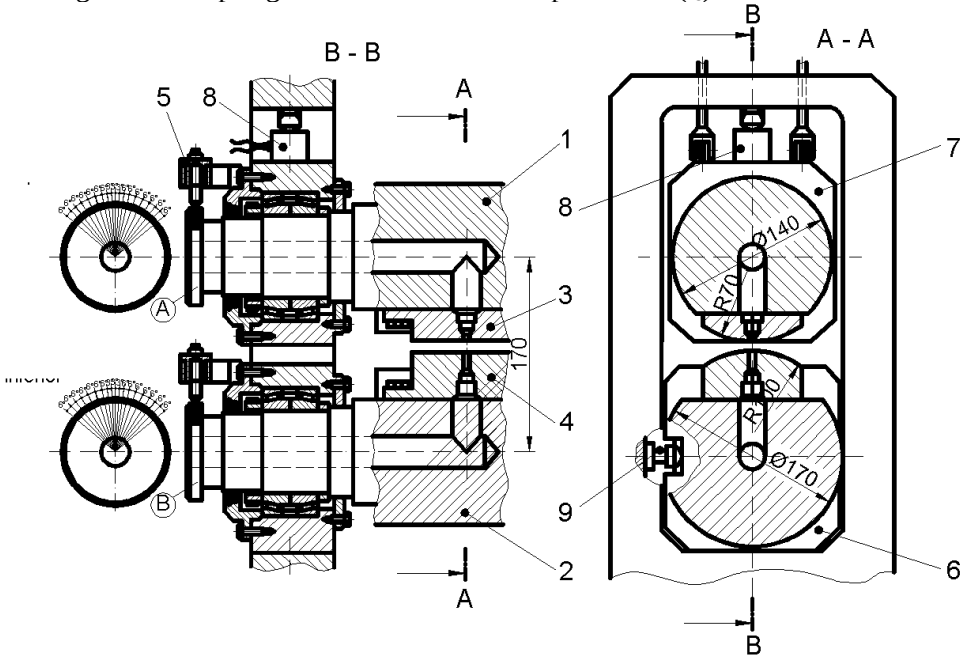

Figure 1. The installation for the research on the force parameters of the symmetric and asymmetric longitudinal rolling process

1 – 140 [mm]- "A" divided head superior roll; **2** – 170 [mm]-"B" divided head inferior roll;
3 – R = 70 [mm] -segment for the superior roll; **4** – R =100 [mm] – segment for the inferior roll;
5 – device for registering the real length of the contact springs; **6 -** bearing
7 – superior roll bearing; **8**– rolling force (F) detector; **9** – side force (X) detector

Since the intended purpose was to study the qualitative aspect of phenomena related to the asymmetric longitudinal rolling, for eliminating the inevitable influence of the iron oxides (scale) on the process, the tests were carried out on samples of aluminum and copper, with the following dimensions [4]:

$$h_0 = 1, 2, 6, 12 \ \ mm$$
$$b_0 = 40\ mm \ \ and \ \ l_0 = 150\ mm$$

In this paper, by analyses and calculations, we are going to use the experimentally obtained values for pressure, and the actual contact lengths of the arcs with the upper and lower roll, for equal diameter and different diameter.

3. Discussions and technological interpretations

Figure 2 shows the dependence of the real length of the contact arc – with the upper roll (smaller) and the lower roll (bigger) – versus the reduction, when rolling the samples whose thicknesses are h_0=12; 6; 2 and 1 mm [4].

As can be seen in the figure, the curves are increasing differently, their points of intersection being found at different degrees of reduction, depending on the thickness of the rolled samples.

Up to the points of intersection (ε=30-35% for h_0 =12 and 6 mm), the length of the arcs afferent to the smaller-diameter roll (upper) is greater, and by further increasing the reduction, the actual lengths of the contact arcs afferent to the smaller-diameter roll become smaller.

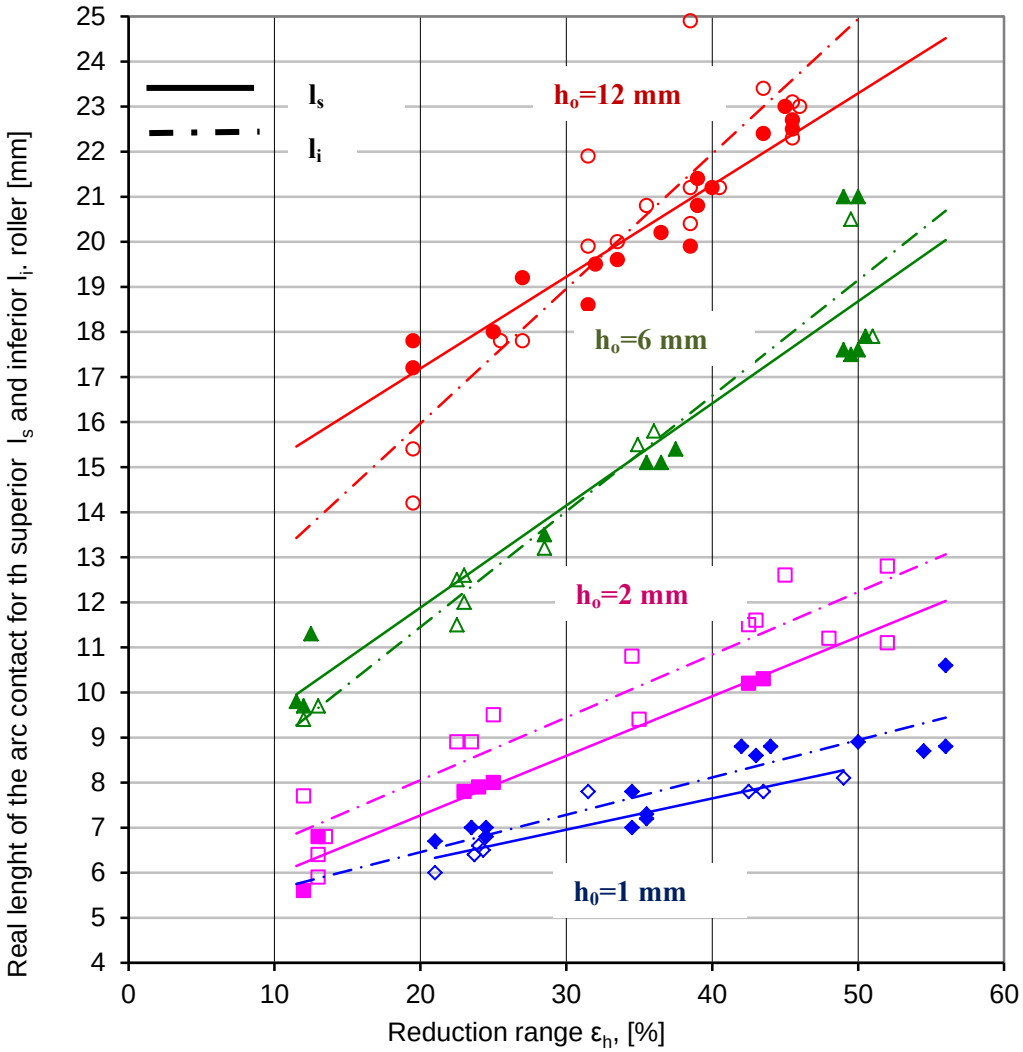

Figure 2. The dependence of the real length of the contact arc – with the upper roll (smaller) and the lower roll (bigger) – versus the reduction, when rolling the samples whose thicknesses are h_0 = 12; 6; 2 and 1 mm

By overlapping the areas where the mean pressure is exerted by the upper roll (smaller) and the lower roll (bigger) for rolling the samples whose dimensions are h_0 =12 mm (Figure 3 and 4), we

discover a similar picture, with the only difference that the chart dependencies for the upper and lower rolls are changing their places, i.e. to the highest values of the length arcs correspond to the lowest pressure values and vice versa.

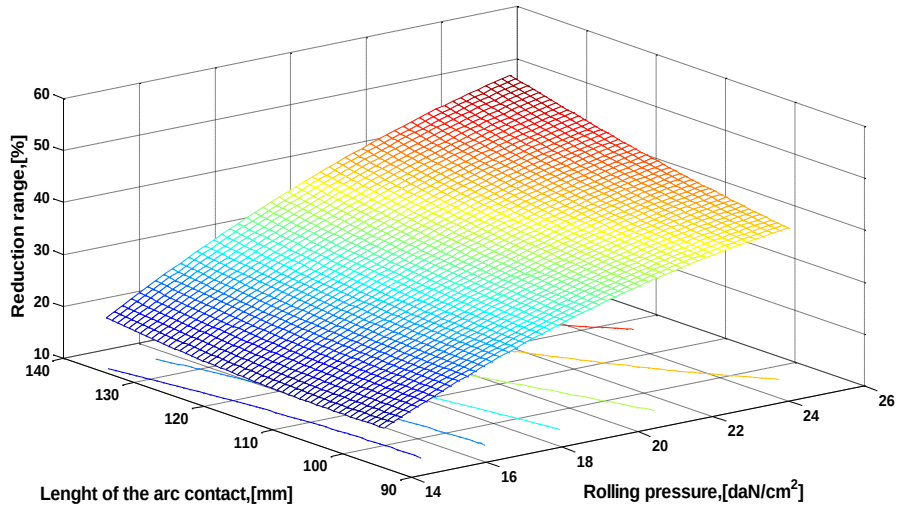

Figure 3. Variation of the rolling pressure and the contact arc length, h_0=12 mm samples between different diameter cylinders $\frac{D_s}{D_i} = \frac{140}{170}$ mm, applying various reductions, lower cylinder

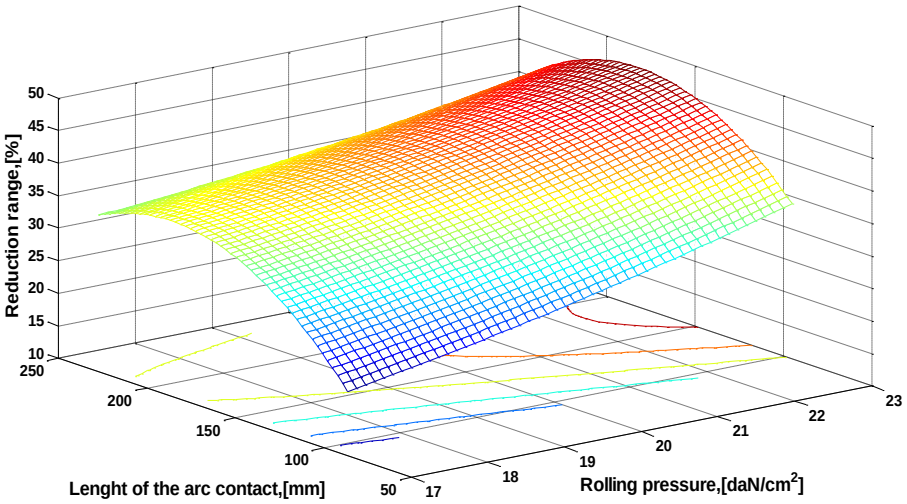

Figure 4. Variation of the rolling pressure and the contact arc length, h_0=12 mm samples between different diameter cylinders $\frac{D_s}{D_i} = \frac{140}{170}$ mm, applying various reductions, upper cylinder

For each thickness, the intersection points of the curves representing the mean pressure and the actual length of the contact arc are placed at the same value of the reduction, confirming the correctness of the experimentally obtained data [5].

For the samples whose dimensions are h_0 = 2 mm (Figure 5 and 6), the intersection points of the curves $l_{rs}=f(\varepsilon, p_{ms})$ and $l_{ri}=f(\varepsilon, p_{mi})$ are moving considerably and correspond to the reduction ε=15-25%, and the length of the contact arcs afferent to the larger-diameter roll (lower) is greater, $l_i > l_s$. It is obvious that, for reductions smaller than the mentioned range, $l_{ri} < l_{rs}$.

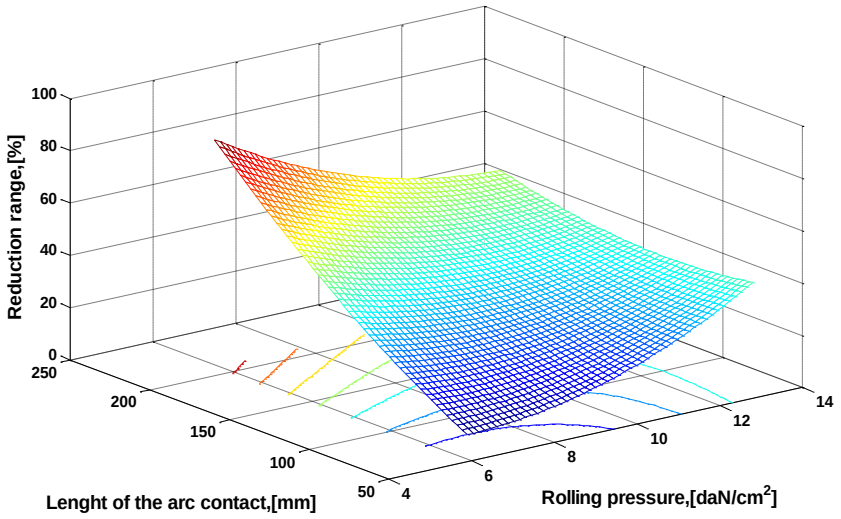

Figure 5. Variation of the rolling pressure and the contact arc length, h_0=2 mm samples between different diameter cylinders $\frac{D_s}{D_i} = \frac{140}{170}$ mm, applying various reductions, lower cylinder

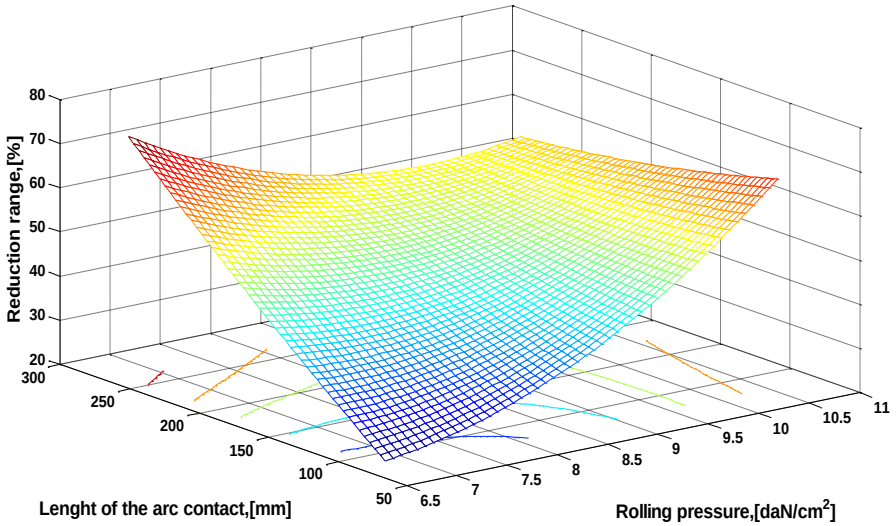

Figure 6. Variation of the rolling pressure and the contact arc length, h_0=2 mm samples between different diameter cylinders $\frac{D_s}{D_i} = \frac{140}{170}$ mm, applying various reductions, upper cylinder

The distribution of the pressure exerted by each roll, for the samples whose dimension is h_0 =2 mm, is shown in Figures 5 and 6. In this case, there is a total concordance with the results presented so far. Therefore, within the reduction range ε =10-25% and $p_{ms} = p_{mi}$.

With increasing degree of reduction, the mean pressure on the smaller-diameter roll (p_{ms}) has a growing value compared to the mean pressure exerted by the larger-diameter roll (p_{mi}).

At reductions smaller than 10-25%, similar to the lengths of the contact arcs, the inequality $p_{mi} > p_{ms}$ is the one which probably applies. The results obtained in the experimental research carried out when using rolls with unequal diameters are fully consistent with the laws of mechanics.

Indeed, for any difference between the diameters of the working rolls and any degree of reduction (ε) applied, $F_s = F_i$, or: $\frac{p_{ms}}{p_{mi}} = \frac{l_i}{l_s}$

Joining the intersection points l_s and l_i shown in Figure 2, for various thicknesses of the rolled samples, as well as the intersection points of the curves describing the mean pressure on the smaller roll (p_{ms}) and the bigger one (p_{mi}) in Figures 3, 4, 5 and 6, we obtain a parabola passing through the origin of the coordinate axes (Figure 7), which in general can be expressed by the equation:

$$y = aX^n \tag{44}$$

where: y – represents the mean pressure (or the lengths of the contact arcs, respectively);
a – coefficient taking into account the rolling conditions;
X – critical degree of deformation;
n – index depending on the degree of asymmetry of the process.

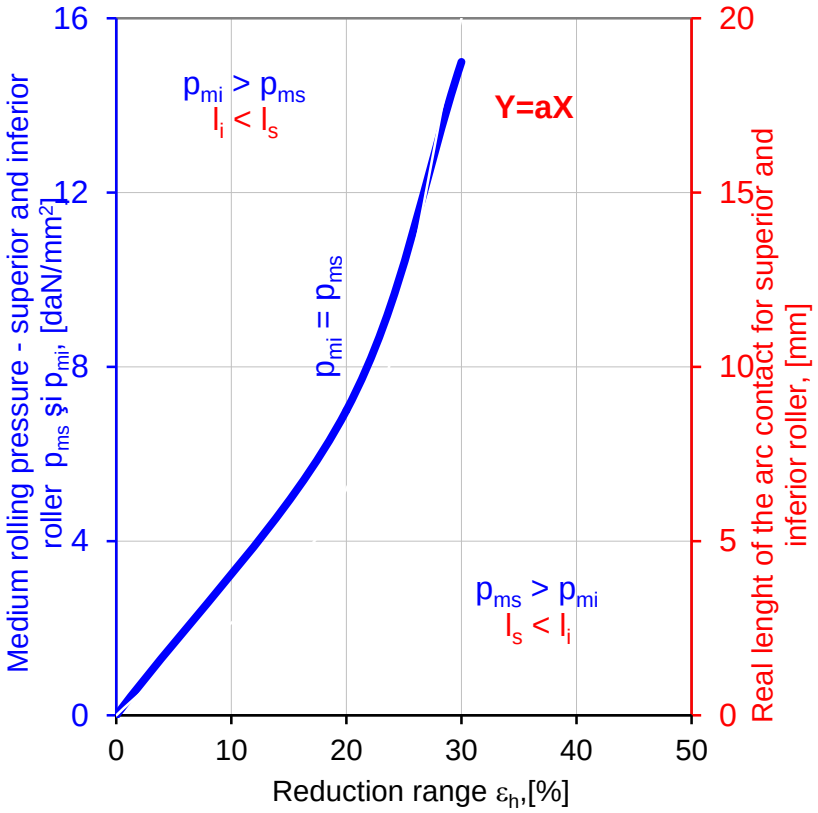

Figure 7. Variation of the rolling pressure and the contact arc length, between different diameter cylinders $\frac{D_s}{D_i} = \frac{140}{170}$ mm, applying various reductions

The obtained curve is in itself the geometrical locus of the points which characterise the partial symmetry conditions of the rolling process between unequal-diameter rolls when the following equalities occur, determining this symmetry:

$$\begin{matrix} p_{ms} = p_{mi} \\ l_s = l_i \end{matrix} \tag{45}$$

In this case, regardless of the ratio between the working diameters of the rolls, the metallic material comes out in a straight line.

The field located above this curve corresponds to the situation when, on the larger-diameter roll (lower), the pressure is higher and the contact arc length is lower, i.e.:

$$\begin{matrix} p_{ms} > p_{mi} \\ l_s < l_i \end{matrix} \tag{46}$$

In this case, all the rolled samples are bending upwards when coming out from the rolls (on the smaller-diameter roll).

The respective field is located under this curve, where the pressure exerted by the smaller-diameter roll (upper) is higher, and the contact arc is shorter:

$$\begin{matrix} p_{ms} < p_{mi} \\ l_s > l_i \end{matrix} \quad (47)$$

In this case, the rolled samples are bending downwards when coming out from the rolls (on the larger-diameter roll). Therefore, in the field located above the curve plotted in Figures 3, 4, 5 and 6, the pressures exerted by the larger-diameter roll are high, and in the field located under the curve, the pressures exerted by the smaller-diameter roll are much higher.

Obviously, when $p_{mi} > p_{ms}$, the bigger is the difference between the working diameters of rolls and the bigger is the initial thickness of the sample, the larger is the field. Related thereto, we should mention that the mean pressure is decreasing with increasing the deformation unevenness.

4. Concluding remarks

The research results confirmed that the current views on the deformation theory, according to which, at asymmetrical rolling, the pressures exerted by the smaller-diameter roll are always higher, are flawed. To characterise the rolling process based on the results obtained from this research, we consider useful to introduce a coefficient able to characterise the degree of asymmetry of the process:

$$K_a = \frac{p_{ms}}{p_{mi}} = \frac{l_i}{l_s} \quad (48)$$

Interpreting the dependencies presented in Figure 7, it results:

If $K_a=1$, this situation corresponds to the case when $y=aX^n$, and characterises the adequate conditions required by a symmetrical process to occur between the unequal-diameter rolls.

The more differs the K_a coefficient from the $K_a=1$ value, the greater is the difference between the contact arc lengths and the mean pressures exerted by the unequal-diameter cylinders, and the more is increasing the degree of unevenness of the deformation.

At the asymmetrical process, when the rolls have unequal diameters, the p_m value is much lower than in case of a symmetrical process under identical conditions of reduction. This phenomenon is fuelled by the denatured shape of the deformation zone, which creates favourable conditions for developing longitudinal tensile stresses, whose action over the bar during the rolling process can match the previous and subsequent stress applied, which considerably reduces the mean pressure exerted on the contact surfaces of the rolls.

References

[1] Alexa V 2002 *Contributions to research asymmetric rolling process*, Politehnica University of Timişoara, Romania, Doctoral Thesis

[2] Alexa V, Ratiu S and Kiss I 2005 Theoretical and experimental analysis of the rolling strain in the deformation area, *Metalurgia International* **5** 20-28

[3] Alexa V, Ratiu S and Kiss I 2016 Metal rolling – Asymmetrical rolling process, *IOP Conf. Ser.: Mater. Sci. Eng.* **106** 012019

[4] Alexa V, Ratiu S and Popa G 2010 *Method and program for automatic calculation forces and momentum to asymmetric longitudinal rolling*, MACMESE'10 Proceedings of the 12th WSEAS international conference on Mathematical and computational methods in science and engineering, Faro, Portugal, November 3-5, pp 303-306

[5] Alexa V 2004 Analysis of the lateral efforts in asymmetrical longitudinal rolling, *Annals of the Faculty of Engineering Hunedoara* **2** 45-50